

## Subdiffusion of a Sticky Particle on a Surface

Q. Xu,<sup>1</sup> L. Feng,<sup>1</sup> R. Sha,<sup>2</sup> N. C. Seeman,<sup>2</sup> and P. M. Chaikin<sup>1</sup>

<sup>1</sup>Center for Soft Matter Research, New York University, New York, New York, 10003, USA

<sup>2</sup>Chemistry Department of New York University, New York, New York, 10003, USA

(Received 17 February 2011; published 2 June 2011)

Conventional diffusion  $\langle \Delta R^2(t) \rangle = 2Dt$  gives way to subdiffusion  $\langle \Delta R^2(t) \rangle \sim t^\mu$ ,  $0 < \mu < 1$  when the waiting time distribution  $\varphi(\tau)$  is nonintegrable. We have studied a model system, colloidal particles functionalized with DNA “sticky ends” diffusing on a complementary coated surface. We observe a crossover from subdiffusive to conventional behavior for  $\langle \Delta R^2(t) \rangle$  and  $\varphi(\tau)$  as temperature is increased near the particle-surface melting temperature consistent with a simple Gaussian distribution of sticky ends. Our results suggest that any system with randomness in its binding energy should exhibit subdiffusive behavior as it unbinds. This will strongly affect the kinetics of self-assembly.

DOI: 10.1103/PhysRevLett.106.228102

PACS numbers: 87.15.Vv

Diffusive processes are of wide interest in understanding various phenomena from the self-assembly materials [1,2] to the kinetics of reaction [3], the migration of large molecules [4], transport in complex networks [5], and protein dynamics [6–8]. Typically diffusive behavior is characterized by the mean squared displacement increasing linearly with time. However, for many physical systems, an anomalous time dependence is found [4,6,7,9–14]. That is,  $\langle \Delta R^2(t) \rangle \sim t^\mu$ , with  $\mu \neq 1$ . As has been analyzed in the continuous random walk model [15,16], subdiffusion ( $\mu < 1$ ) may arise when there is a broad distribution of local waiting times,  $\varphi(\tau) \sim \tau^{-(1+\mu)}$ , while superdiffusion ( $\mu > 1$ ) corresponds to long-range correlations in velocities or “Levy flights.” Although mechanisms for anomalous diffusion have been studied theoretically and numerically, there have been few experimental tests of subdiffusion where displacements and waiting times are experimentally measured and compared with a theoretical model. In this Letter, we present an investigation of a model system: colloidal particles functionalized with DNA “sticky ends” on a flat substrate with complementary DNA sticky ends. Licata and Tkachenko analyzed such systems and found complex behavior including subdiffusion. Moreover, this colloidal system with its specific reversible bonds is often used for self-assembly where the kinetics, often slow relaxational kinetics, are important to understand both the formation process and the final structures [17–22]. A basic question for complex self-assembly is how particles diffuse on each other’s surface once they are bound and how long the system should be allowed to equilibrate.

A schematic of the experimental geometry is shown in Fig. 1. The DNA used contains 61 nucleotides (ordered from IDT, Coralville, IA), hybridized from its 5’ end with complementary DNA strands including 49 nucleotides, leaving one base as a hinge and 11 unpaired bases for use as “sticky ends.” The particles used in the study are 1.05  $\mu\text{m}$  streptavidin-coated beads (density  $\sim 2.2 \times$

$10^3 \text{ kg/m}^3$ ) purchased from Invitrogen and the substrate is a silicon wafer coated with 5 nm Cr and 20 nm Au. The DNA strands (labeled as C in Fig. 1) are connected at the 5’ end to a TEG (triethylene glycol) spacer terminated by a biotin group which attaches to the streptavidin on the particles. The complementary DNA strands (C’ sequence) have a TEG spacer attached to a thiol group which binds to the Au surface. The coverage of the surfaces was measured by radioactive labeling ( $^{32}\text{P}$ ) tracer DNAs. This determination shows that the average spacing between strands on the particle and gold surfaces is about 12 and 18 nm, respectively. The entire preparation process was performed in the buffer (pH 7.5) with a total concentration of 10 mM phosphate, 50 mM NaCl, and 0.5% w/w Pluronic

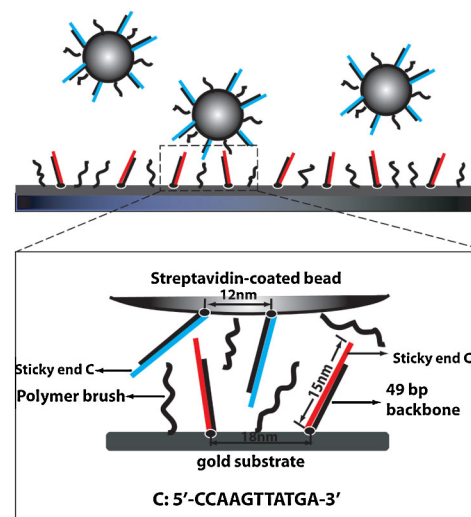


FIG. 1 (color online). Schematic representation of our experimental system, consisting of 1.05  $\mu\text{m}$  diameter streptavidin-coated beads and a gold surface (30 nm in thickness), both of which are covered by short ( $h \sim 15 \text{ nm}$ ) complementary DNA strands (C/C’). A sterically stabilizing polymer brush prevents nonspecific binding between particles and surface.

surfactant (F108, the Polymer brush shown in the Fig. 1). The particles are heavy so that their motion is confined in the region near the bottom plane. Therefore, the system can be treated as two-dimensional in our experiments.

The aggregation of complementary DNA-functionalized colloids is well described in Refs. [19,20] and characterized by the fraction of singlet, unpaired particles as a function of temperature. Here we adapt a similar convention and plot the melting curve, Fig. 2(a), for particle-substrate binding as the fraction of moving particles. “Moving” is defined as a displacement larger than 50 nm (1 pixel) between frames (frame rate = 1 Hz). The free energy of a single tethered DNA bond is  $\Delta F_{\text{tether}} = \Delta H_0 - T\Delta S_0 - T\Delta S_p$ , with  $\Delta H_0 = -322.4$  kJ/molK,  $\Delta S_0 = -935.6$  J/molK for the sequence we used [23], and  $\Delta S_p$  is the entropy loss due to the restriction of its motion when joining the surface between beads [24,25]. The binding free energy of the bead is therefore

$$\Delta F_{\text{bead}} = -RT \ln[(1 + ke^{-\Delta F_{\text{tether}}/RT})^{N_b} - 1], \quad (1)$$

where  $N_b$  is the maximum number of bridges which can form between surfaces and  $k$  indicates the number of bonds that opposing sticky ends can reach. A simple geometrical estimate [20] gives  $N_b \approx 150$  and  $k \approx 13$  for our configuration. The solid line in Fig. 2(a) is a model fit (the expression given in Ref. [26]) using  $\Delta S_p = -14.76R$ .

Displacement vs time measurements were taken by tracking individual particles with a microscope (Qimage Retiga 1300 camera on a Leica microscope  $100\times$ , 50 nm pixel size) over the temperature range 43–47 °C. Care was taken to avoid any slow drift of the camera during our observation. The sample is restrictedly sealed from the atmosphere so that there is no external flow and evaporation of the solution. Specific trajectories at 44.1 °C, 44.3 °C, 44.5 °C, and 44.7 °C are shown in Fig. 2(c). At each temperature 10 different particles trajectories were measured from 10 s to 10 h. For all the temperatures, the experiments were repeated for 10 separate samples. At temperatures above the melting temperature of 45 °C, Fig. 2(a), conventional diffusion was observed with  $D_{47^\circ\text{C}} = \langle \Delta r^2(t)/4t \rangle \approx (0.38 \pm 0.02) \mu\text{m}^2/\text{s}$ . This value is about 56% of the free diffusion ( $D_f$ ) value due to hydrodynamic proximity of the surface. At 44.7 °C, the diffusion constant is greatly reduced,  $D_{44.7^\circ\text{C}} \approx 1.4 \times 10^{-3} \mu\text{m}^2/\text{s} \sim D_{47^\circ\text{C}}/270$  but diffusion is still conventional,  $\langle \Delta r^2(t) \rangle \propto t$ . At this temperature, the particle is bound by DNA hybridization to the surface for a certain waiting time  $\tau$ , escapes from the surface and diffuses freely for an average time,  $\tau_{\text{free}} \sim 0.4$  s, an average stepsize,  $l \sim \sqrt{D_{47^\circ\text{C}}\tau_{\text{free}}} \sim 0.8 \mu\text{m}$ , and then rebinds to the surface. The characteristic distance  $l \sim h_g = k_B T/mg$  is the gravitational height. Therefore, in our system diffusion is governed by a well defined stepsize  $h$  and a temperature dependent distribution of waiting times,  $\tau$ . If  $\langle \tau \rangle$  exists,  $D \approx h_g^2 / \langle \tau \rangle$ . On further lowering the temperature the DNA binding becomes more important and as the waiting time increases the ensemble-averaged mean squared displacement becomes subdiffusive. A power-law fit to the experimental results gives  $\mu = 0.35 \pm 0.02$ ,  $0.53 \pm 0.02$ ,  $0.78 \pm 0.03$  as  $T = 44.1^\circ\text{C}$ ,  $44.3^\circ\text{C}$ ,  $44.5^\circ\text{C}$  [Fig. 2(b)]. In this regime, mobility decreases precipitously as temperature is lowered and the dynamics is remarkably slowed down. The fact that the residence time  $\tau$  in the “traps” becomes very long compared to  $\langle \tau_{\text{free}} \rangle$  allows us to treat our system with a standard continuous random walk model in this temperature range. For  $T < 44.1^\circ\text{C}$ , the probability for particles to desorb from the surface is too small to distinguish any significant motion.

Intrinsically, subdiffusive behavior is related to the waiting time,  $\tau$ , before each step. In these experiments we have measured the waiting time along with the displacement for all particle trajectories. Again we use a simple protocol that a particle is not moving if its displacement is less than 50 nm (1 pixel). Here, we recorded  $\tau$  of each step during

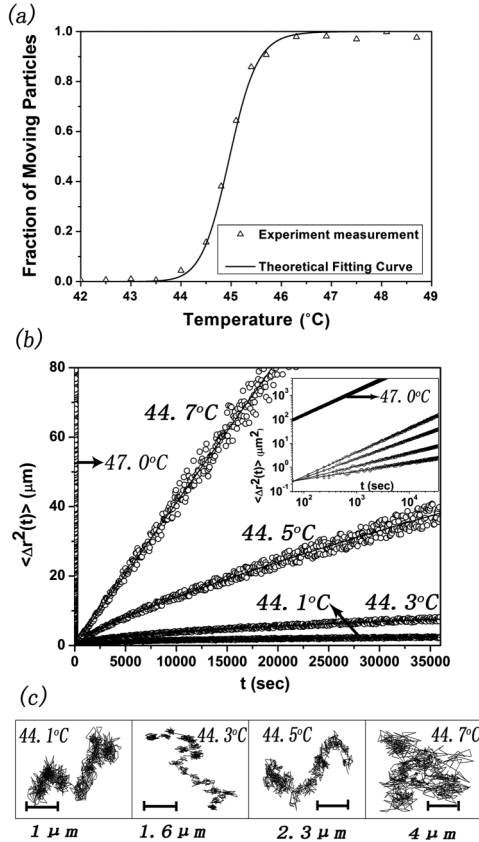


FIG. 2. Experiment results. (a) The fraction of moving particles as a function of temperature. The triangles are the experiment data and the solid black line is the best fitting curve choosing  $\Delta S_p = -14.76R$ . (b) Ensemble-averaged mean squared displacement varies with temperature. The solid lines indicate power-law fits. Consequently,  $\mu = 0.35 \pm 0.02$  ( $T = 44.1^\circ\text{C}$ ),  $0.53 \pm 0.02$  ( $T = 44.3^\circ\text{C}$ ),  $0.78 \pm 0.03$  ( $T = 44.5^\circ\text{C}$ ),  $0.99 \pm 0.03$  ( $T = 44.7^\circ\text{C}$ ) (curves from bottom to top). (c) The trajectories of the same particle over 10 hours at  $T = 44.1^\circ\text{C}$ ,  $44.3^\circ\text{C}$ ,  $44.5^\circ\text{C}$ ,  $44.7^\circ\text{C}$ .

the diffusion process for every single particle, which statistically gives the likelihood of a particle sitting in a position for time  $\tau$  before performing the next jump. The results can be further converted into probability density distribution of trapping time,  $\varphi(\tau)$ , which is shown in Fig. 3 for the four temperatures studied. The log-log plots show good fits to power laws  $\varphi(\tau) \sim \tau^{-(1+\mu')}$  with  $\mu' = 0.32, 0.55, 0.73, 1.00$ , respectively.

Generally, if the number of bonds ( $N_b$ ) formed between a particle and surface is constant for a fixed geometry, the characteristic time for this particle to stick on the surface is given by  $\bar{\tau}(N_b, T) = \frac{1}{\omega} \exp[-\Delta F_{\text{bead}}(N_b, T)/k_B T]$ . Here the escape attempt frequency  $\omega \sim \frac{D_f}{Rh \ln(R/h)} \sim 20$  Hz, which is the inverse of time to diffuse a DNA bond length ( $h \sim 15$  nm) [27]. However, in our experiment, where the particle explores the DNA covered substrate, the number of bonds  $N_b$  varies for each particle-surface configuration due to shape and coverage heterogeneities. Thus, instead of treating  $N_b$  as constant, it is more reasonable to introduce a statistical distribution  $\rho(N_b)$  for the probability of  $N_b$  bonds connecting particle to surface. For each  $N_b$ , there is a characteristic time  $\bar{\tau}(N_b, T)$  as above and the unbinding is a Poisson process with the probability of survival at time  $\tau$ :  $P_s(\tau) \approx e^{-\tau/\bar{\tau}(N_b, T)}$ . For a normalized distribution of bond numbers  $\rho(N_b)$ , this probability becomes  $P(\tau, T) = \sum_{N_b \neq 0} \rho(N_b) e^{-\tau/\bar{\tau}(N_b, T)}$  and

$$\varphi(\tau, T) = -\frac{dP(\tau, T)}{d\tau} = \sum_{N_b=0} \frac{\rho(N_b)}{\bar{\tau}(N_b, T)} \exp\left(-\frac{\tau}{\bar{\tau}(N_b, T)}\right). \quad (2)$$

$\varphi(\tau)\Delta\tau$  gives the escape probability during the interval  $\tau \rightarrow \tau + \Delta\tau$ . Assuming that the heterogeneities in particle and surface coverage are uncorrelated, we take  $\rho(N_b)$  as a Gaussian distribution  $\rho(N_b) = \frac{1}{\sqrt{2\pi\sigma^2}} \exp(-\frac{(N_b - \bar{N})^2}{2\sigma^2})$  with the mean value  $\bar{N}$  and variance  $\sigma$ . Here, the mean number of the contacts is determined by our radioactive trace measurement:  $\bar{N} \approx 150$ . Therefore, the distribution has

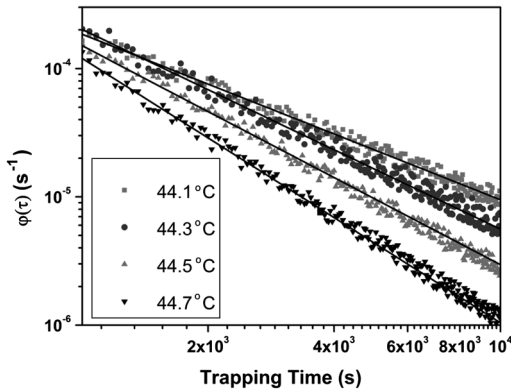


FIG. 3. Distribution of trapping time  $\tau$ . The solid black lines indicate the power-law fits to the experimental results of escape probability  $\varphi(\tau)$  with  $\mu' = 0.32, 0.55, 0.73, 1.00$ .

only one unknown, the variance  $\sigma$ , which can be adjusted to the data. In Fig. 4(a) we show the calculated and measured  $\varphi(\tau)$  superposed where a least squares fit was used to obtain  $\sigma = 29.8 \pm 0.04$  [28]. Why does this work so well given that our  $\varphi(\tau)$  [Eq. (2)] is not an obvious power law? In Fig. 4(b), we plot  $\varphi(\tau)$  for the temperature range of interest on log-log scales. It is clear that over the region of experimental interest 1000–10 000 s the function  $\varphi(\tau, T)$  is well fit (correlation = 0.998) by a power law. Here,  $\mu_{\text{fit}}^{\text{Calc}} = 0.33, 0.54, 0.79, 1.09$  for  $T = 44.1^\circ\text{C}, 44.3^\circ\text{C}, 44.5^\circ\text{C}, 44.7^\circ\text{C}$ .

In random walk theory, subdiffusion occurs when the average waiting time diverges,  $\langle\tau_{\text{aver}}\rangle \sim \int_0^\infty \tau \tau^{-(1+\mu)} d\tau \rightarrow \infty$  ( $\mu < 1$ ). Finite  $\langle\tau_{\text{aver}}\rangle$  gives linear diffusion. Nevertheless, our statistical model indicates that [from Eq. (2)]

$$\begin{aligned} \langle\tau_{\text{aver}}\rangle &= \int_0^\infty \tau \varphi(\tau) d\tau \\ &= \frac{1}{\omega} \sum_{N_b=0} \rho(N_b) [(1 + k e^{-\Delta F_{\text{bead}}/k_B T})^{N_b} - 1] \quad (3) \end{aligned}$$

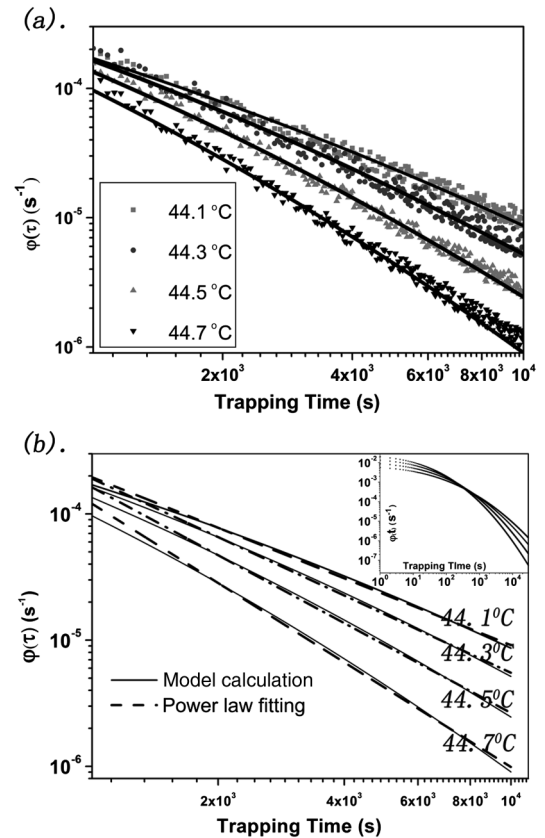


FIG. 4. (a) Comparison between experimental results and model calculation of escape probability  $\varphi(\tau)$  at temperature  $T = 44.1^\circ\text{C}, 44.3^\circ\text{C}, 44.5^\circ\text{C}, 44.7^\circ\text{C}$ . (b) Calculated trapping time distribution  $\varphi(\tau)$  and least squares power-law fits for the same temperatures as in (a). Fit exponents are  $\mu_{\text{fit}}^{\text{Calc}} = 0.33, 0.54, 0.79, 1.09$ , respectively. Inset plot is  $\varphi(\tau, T)$  for the time range  $10^1 \text{ s} \sim 3 \times 10^4 \text{ s}$ .

so that  $\langle\tau_{\text{aver}}\rangle$  remains finite. If we wait long enough, the particles must eventually exhibit conventional diffusion. If  $\langle\tau_{\text{aver}}\rangle$  is much longer than the total observation time ( $\tau_{\text{total}} \sim 10$  h), the particle will not explore the end of the power-law tail of  $\varphi(\tau, T)$ . Thus, the subdiffusive behavior in this experiment happens only for a comparatively short observation time during which the particles are not in equilibrium. It is interesting to ask how many  $\langle\tau_{\text{aver}}\rangle$  one has to wait before getting conventional “equilibrium” diffusion rather than subdiffusion. Since our experimental  $\langle\tau_{\text{aver}}\rangle$  depends on  $T$ , we can observe this crossover simply by increasing the temperature. For  $T = 44.1^\circ\text{C}$ ,  $44.3^\circ\text{C}$ ,  $44.5^\circ\text{C}$ ,  $\tau_{\text{aver}} = 1.32 \times 10^6$  s,  $3.10 \times 10^5$  s,  $8.25 \times 10^4$  s, respectively, all of which are longer than  $\tau_{\text{total}}$  and exhibit subdiffusion. But for  $T = 44.7^\circ$ ,  $\tau_{\text{aver}} = 2.5 \times 10^4$  s  $<$   $t_{\text{total}} \sim 3 \times 10^4$  s and we observe conventional diffusion.

In summary, we have observed subdiffusion and a crossover to conventional diffusion in a model system of sticky particles made from DNA-functionalized colloids and a complementary DNA coated surface. We show theoretically that the subdiffusion results from a distribution of local waiting times related to a Gaussian distribution of binding energies and Poisson statistics. This is useful directly for studying the kinetics of DNA-based self-assembly and particularly its temperature dependence. However, the fact that almost all “sticky” systems have some Gaussian randomness in their binding energies suggests that subdiffusion should be ubiquitous over a temperature range near the dissociation point. We find that the crossover to conventional diffusion occurs as soon as the measurement time is longer than the average escape time.

We thank Professor A. Grosberg, Dr. A. V. Tkachenko, and Dr. R. Dreyfus for useful discussions. The work is partially supported by the Keck Foundation, by NSF through the NYU MRSEC DMR-0820341, and by NASA NNX08AK04G.

- 
- [1] N. A. Licata and A. V. Tkachenko, *Europhys. Lett.* **81**, 48 009 (2008).
  - [2] N. A. Licata and A. V. Tkachenko, *Phys. Rev. E* **74**, 041408 (2006).
  - [3] H. Berry, *Biophys. J.* **83**, 1891 (2002).
  - [4] M. Schunack, T. R. Linderoth, F. Rosei, E. Laegsgaard, I. Stensgaard, and F. Besenbacher, *Phys. Rev. Lett.* **88**, 156102 (2002).
  - [5] C. Nicolaidis, L. Cueto-Felgueroso, and R. Juanes, *Phys. Rev. E* **82**, 055101 (2010).
  - [6] D. S. Banks and C. Fradin, *Biophys. J.* **89**, 2960 (2005).
  - [7] I. Y. Wong, M. L. Gardel, D. R. Reichman, E. R. Weeks, M. T. Valentine, A. R. Bausch, and D. A. Weitz, *Phys. Rev. Lett.* **92**, 178101 (2004).
  - [8] M. C. Konopka, I. A. Shkel, and J. C. Weisshaar, *J. Bacteriol.* **188**, 6115 (2006).

- [9] T. H. Solomon, E. R. Weeks, and H. L. Swinney, *Phys. Rev. Lett.* **71**, 3975 (1993).
- [10] J. Bernasconi, S. Alexander, and R. Orbach, *Phys. Rev. Lett.* **41**, 185 (1978).
- [11] A. Stanislavsky and K. Weron, *Phys. Rev. E* **82**, 051120 (2010).
- [12] D. Brockmann and T. Geisel, *Phys. Rev. Lett.* **90**, 170601 (2003).
- [13] L. F. Richardson, *Proc. R. Soc. A* **110**, 709 (1926).
- [14] M. F. Shlesinger, G. M. Zaslavsky, and J. Klafter, *Nature (London)* **363**, 31 (1993).
- [15] A. Ott, J. P. Bouchaud, D. Langevin, and W. Urbach, *Phys. Rev. Lett.* **65**, 2201 (1990).
- [16] J. P. Bouchaud and A. Georges, *Phys. Rep.* **195**, 127 (1990).
- [17] A. V. Tkachenko, *Phys. Rev. Lett.* **89**, 148303 (2002).
- [18] S. Y. Park, A. K. R. Lytton-Jean, S. Weigand, B. Lee, G. C. Schatz, and C. A. Mirkin, *Nature (London)* **451**, 553 (2008).
- [19] P. L. Biancaniello, A. J. Kim, and J. C. Crocker, *Phys. Rev. Lett.* **94**, 058302 (2005).
- [20] M. P. Valignat, O. Theodoly, J. C. Crocker, W. B. Russel, and P. M. Chaikin, *Proc. Natl. Acad. Sci. U.S.A.* **102**, 4225 (2005).
- [21] D. Nykypanchuk, M. M. Maye, D. van der Lelie, and O. Gang, *Nature (London)* **451**, 549 (2008).
- [22] M. E. Leunissen, R. Dreyfus, R. Sha, T. Wang, N. C. Seeman, D. J. Pine, and P. M. Chaikin, *Soft Matter* **5**, 2422 (2009).
- [23] J. SantaLucia, *Proc. Natl. Acad. Sci. U.S.A.* **95**, 1460 (1998).
- [24] R. Dreyfus, M. E. Leunissen, R. Sha, A. V. Tkachenko, N. C. Seeman, D. J. Pine, and P. M. Chaikin, *Phys. Rev. Lett.* **102**, 048301 (2009).
- [25] R. Dreyfus, M. E. Leunissen, R. Sha, A. Tkachenko, N. C. Seeman, D. J. Pine, and P. M. Chaikin, *Phys. Rev. E* **81**, 041404 (2010).
- [26] Equating the chemical potential of free and absorbed particles, the fraction of unbound particles is  $f = \frac{(C_b - C_f)K - 1 + \sqrt{1 + 2(C_f + C_b)K + (C_f - C_b)^2 K^2}}{2KC_b}$  where  $C_f (\sim 20/\mu\text{m}^2)$  is the surface concentration of absorbing sites and  $C_b (\sim 0.1/\mu\text{m}^2)$  is the concentration of particles. The equilibrium constant is  $K \approx A_\omega \exp(-\Delta F_{\text{bead}}/RT)$  with  $A_\omega \sim 9 \text{ nm}^2$  for our system (see Ref. [19]).
- [27] When the particles are at a height  $x$  from the surface, hydrodynamics reduce the diffusion coefficient to  $D(x) = D_f \frac{x}{R}$  ( $R$  the particle radius). W. B. Russel, D. A. Saville, and W. R. Schowalter, in *Colloidal Dispersions* (Cambridge University Press, Cambridge, England, 1989) p. 44) Assuming that  $c(x)$  vanishes at  $\sim R \gg h$  and escape flux  $J = -D(x) \nabla c(x)$ , we obtain  $c(h) \sim \frac{JR}{D_f} \ln \frac{R}{h}$  for steady states. The attempt escape frequency is then  $\omega = -\frac{dn/dt}{n} = \frac{J}{c(h)h} \sim \frac{D_f}{Rh \ln(R/h)}$ .
- [28] One might expect  $\sigma \sim \sqrt{N} \sim 12$ , rather than our value of  $\sim 30$ . We suspect that the roughness of our beads contributes to the variance in the area of contact with the surface.